Available online at www.sciencedirect.com

ScienceDirect

Proceedings of the Combustion Institute 000 (2020) 1–9

Proceedings of the Combustion Institute

www.elsevier.com/locate/proci

Experimental and numerical investigation of temperature fluctuations in the near-wall region of an optical reciprocating engine ☆

Mohammad K. Alzuabi*, Angela Wu, Volker Sick

Department of Mechanical Engineering, the University of Michigan, Ann Arbor, MI, USA

Received 7 November 2019; accepted 31 August 2020
Available online xxx

Abstract

Accurate prediction of in-cylinder heat transfer processes within internal combustion engines (ICEs) requires a comprehensive understanding of the boundary layer effects in the near-wall region (NWR). This study investigates near-wall temperature fluctuations of an optical reciprocating engine using a combined approach of planar laser-induced fluorescence (PLIF) thermometry and numerical conjugate heat transfer modeling. Single-line excitation of toluene and subsequent one-color emission detection is employed for PLIF thermometry, while large-eddy simulations (LES) using commercial CFD software (CONVERGE v2.4.18) is utilized for modeling. The PLIF signal is calibrated to predicted in-cylinder temperatures from a GT-POWER simulation, and precision uncertainty of temperature is found to be ±1.5 K within the calibration region. Near-wall temperature fluctuations are determined about the multi-cycle mean, and the development of thermal stratification is captured in the NWR under motored and fired conditions during the compression stroke. Regions of the largest cycle-to-cycle temperature fluctuations are identified closer to the in-cylinder head surface indicating the unsteadiness of the thermal boundary layer. Analysis includes an assessment of cyclic variability of near-wall temperature fluctuation, and the effects of compression on temperature fluctuations. Additionally, thermal stratification is found to be similar under motored and fired conditions before ignition timing. Lastly, spatial correlation analysis of temperature fluctuations is performed in the wall-normal direction, and it reveals higher correlations under fired conditions. Spatial correlations experience an initial drop outside of the buffer layer in the NWR, and the location of the drop is well captured in the simulations. Analysis of fluctuating temperatures needs to be extended to fluctuations about the spatial average temperature which directly affects the spatial thermal gradients relevant to engine heat transfer.

Keywords: PLIF Thermometry; LES; Conjugate heat transfer; Near-wall region; Optical engine

1. Introduction

Heat transfer plays a dominant role in the design and development of internal combustion engines (ICEs). It causes changes in gas

☆ Colloquium that describes the research topic: Reciprocating internal combustion engines.

* Corresponding author.
E-mail address: malzuabi@umich.edu (M.K. Alzuabi).

https://doi.org/10.1016/j.proci.2020.08.062
1540-7489 © 2020 Published by Elsevier Inc. on behalf of The Combustion Institute.

temperature that directly affect the engine's performance, efficiency, and emissions. In particular, local temperature gradients near the end of the compression stroke dictate flame propagation, and could cause auto-ignition [1,2]. Thus, accurately predicting engine heat transfer is essential for computational design of advanced combustion strategies for clean and efficient engines, but it is critically dependent on modeling the near-wall region (NWR) [3,4]. However, the lack of a detailed experimental characterization of the dynamic NWR and challenges in modeling its unsteady and turbulent nature have limited the development of more accurate engine heat transfer models.

Laser-based and other optical diagnostics have enabled research to investigate thermal stratification in the in-cylinder core region, but only a few studies examined the NWR. Lucht and Maris [5] reported coherent anti-Stokes scattering (CARS) measurements of near-wall burned gas temperatures in an engine, which showed thickening of the thermal boundary layer during the expansion stroke. Lucht et al. [6] studied the effect of swirl motion on temperature profiles and measured wall heat transfer at the CARS measurement location corresponding to velocity data reported in [7]. These single-point CARS measurements were valuable, but provided limited insights on the spatial and temporal development of the thermal boundary layer. Dec and Hwang [8] characterized the evolution of thermal stratification in a homogenous-charge compression-ignition (HCCI) engine using planar laser-induced fluorescence (PLIF), and identified distinct hotter and colder regions with a turbulent structure late in the compression stroke. Snyder et al. [9] investigated thermal stratification under fired conditions, and found its distribution and development similar to the motored conditions. Dronniou and Dec [10] analyzed the development of thermal stratification from the NWR to the bulk-gas, and found it was caused by cold turbulent structures extending from the in-cylinder head and piston surfaces. Additionally, Cundy and Sick [11] performed a higher-resolution experiment to identify thermal boundary layer structures in ICEs, but they only reported qualitative results of spatial and temporal variations near the wall due to limited signal-to-noise ratio (SNR). Kaiser et al. [12] measured spatial temperature fluctuations in the compression stroke, and noticed greater inhomogeneities confined near the walls. Peterson et al. [13,14] used high-speed PLIF thermometry combined with particle image velocimetry (PIV) to investigate the development of natural thermal stratification, and noticed significant increase in stratification during expansion. These studies laid the ground for further experiments of higher spatial and temporal resolution in order to capture the thermal boundary layer effects.

Thermal boundary conditions have often been overlooked in computational fluid dynamics (CFD) engine simulations. Experimental measurements revealed significant spatial and temporal variation of the engine wall temperature [15], but typical wall modeling uses uniform and constant thermal boundary conditions. Conjugate heat transfer (CHT) modeling is necessary to define the thermal boundary conditions more accurately. Misdariis et al. [16] coupled large-eddy simulations (LES) with CHT to better predict engine heat transfer, but neglected moving geometries. Wu et al. [17] improved the CHT methodology by including moving solid components in their LES, which enabled them to capture substantial spatial, temporal, and cyclic variability in the wall heat transfer.

Moreover, spatial correlations of temperature fluctuations in ICEs have not been explored as extensively as velocity fluctuations despite their significance to engine heat transfer [18,19]. These correlations provide an indication of temperature length scales and thermal gradients. Schmitt et al. [20,21] studied an engine-like flow using direct numerical simulations (DNS), and calculated the temperature length scales during the compression stroke. They found that the length scale decreases towards the wall due to larger thermal gradients.

The present work uses a combined approach of experimental toluene-PLIF thermometry and numerical CHT modeling [17] to further investigate temperature fluctuations in the NWR of an optical reciprocating engine. It presents instantaneous images of near-wall temperature fluctuations under motored and fired conditions and the location of the highest fluctuations during the compression stroke. Moreover, it explores the experimental and numerical temperature cycle-to-cycle variability (CCV), and the evolution of fluctuating thermal stratification in the NWR. Lastly, it examines the spatial correlations of temperature fluctuations in the wall-normal direction to provide an indication of their spatial scales. This is an important step towards addressing the critical need to characterize the thermal boundary layer structure behavior within ICEs.

2. Experimental method

Measurements of temperature distributions were conducted in the NWR of the TCC-III engine described in [22,23]. It is a two-valve, four-stroke, single cylinder, pancake-shape chamber engine with a centrally-installed spark plug in the cylinder head. Optical access is achieved through the quartz cylinder liner and flat piston window. Operating parameters and engine details are shown in Table 1. The crank-angle degree (CAD) definition assigns 0 CAD to top-dead center compression (TDCc).

High-speed toluene PLIF thermometry was conducted to capture temperature variations in an

Please cite this article as: M.K. Alzuabi, A. Wu and V. Sick, Experimental and numerical investigation of temperature fluctuations in the near-wall region of an optical reciprocating engine, Proceedings of the Combustion Institute, https://doi.org/10.1016/j.proci.2020.08.062

Table 1
Engine parameters and operating conditions.

Parameter	Value
Engine speed	1300 rpm
Engine bore, stroke	92, 86 mm
Clearance height at TDC	9.5 mm
Geometric compression ratio	10:1
Intake, exhaust pressure	40, 95 kPa
Engine oil and coolant temp.	353.15 K
Intake temperature	353.15 K
Intake valve closing (IVC)	−120 CAD
Ignition timing	−18 CAD
Toluene tracer seeding	5% by vol
Fuel, stoichiometric ratio	Propane, 1

$8 \times 6\ mm^2$ field-of-view (FoV) adjacent to the cylinder head surface, with simultaneous measurements of surface temperature and heat flux via a heat transfer probe, positioned 35.5 mm from the cylinder axis, as shown in Fig. 1. The diagnostic is implemented using a Scheimpflug adapter that allowed a tilted imaging setup to better enable imaging in the near-wall proximity as discussed in [19,23,24]. Toluene was premixed with heated air upstream of the intake plenum using a high-performance liquid chromatography (HPLC) pump. A diode-pumped Nd:YAG laser (Hawk-HP, Continuum) provided 266 nm pulsed light of 1 mJ. A laser beam was formed into a 1 mm thick and 10 mm wide light sheet at the measurement location by a combination of spherical and cylindrical lenses. The laser sheet was reflected off a 45° mirror inside the engine crankcase to pass through the quartz-bottom piston window, illuminating a vertical viewing plane.

A one-color detection technique was used for the toluene-PLIF imaging with a setup similar to [8,12,25]. Fluorescence signal was collected with a UV lens (Halle, $f = 100$ mm, $f/2$) attached to a two-stage intensified relay optics (HS-IRO, LaVision) coupled to a high-speed 14-bit CMOS camera (Phantom v7.3). The signal passed through two 275 nm long-pass (LP) filters and a 350 nm short-pass (SP) filter. An optical crank-angle encoder (AVL) was used to synchronize the laser and camera at about 6 kHz, and timings of the laser pulse and camera acquisition were controlled by a high-speed controller (HSC, LaVision). PLIF images at every 1.3 CAD were recorded for 73 and 145 consecutive cycles under motored and fired conditions, respectively, performed with continuous firing. The in-plane spatial resolution of the PLIF detection system was determined with a 1951 USAF resolution target to be approximately 0.1 mm. The distance in the wall-parallel and wall-normal direction is denoted by x_{Head} and y_{Head}, respectively.

PLIF images from the one-color detection technique require substantial post-processing steps before deriving quantitative information [26]. These include corrections for variations in pulse-to-pulse laser energy, background fluorescence, tracer density number changes with crank angle, light attenuation and other image non-uniformities due to beam profile and steering [8,10,12,14]. This work followed the flat-field correction (FFC) method [8,12,13]. Instantaneous PLIF images were first normalized by reference laser energy readings before subtracting the background and being normalized by a reference toluene number density at intake valve closing (IVC). Then, a normalization by the

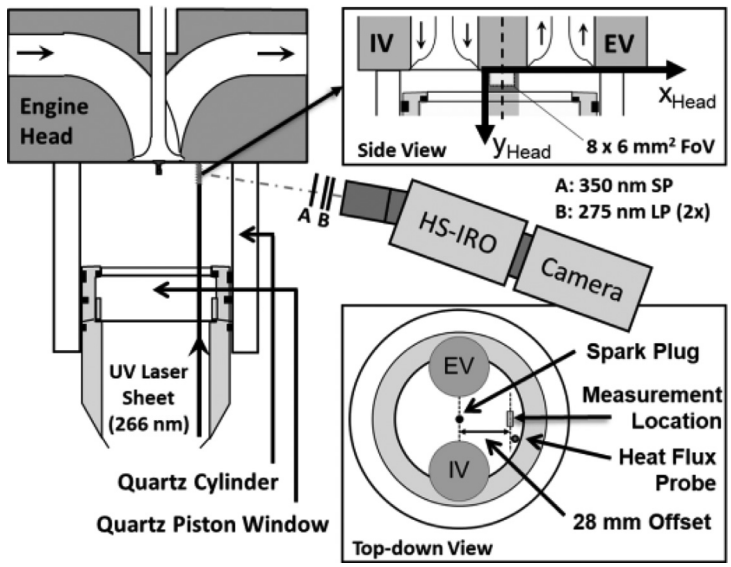

Fig. 1. Schematic of the TCC-III engine.

Please cite this article as: M.K. Alzuabi, A. Wu and V. Sick, Experimental and numerical investigation of temperature fluctuations in the near-wall region of an optical reciprocating engine, Proceedings of the Combustion Institute, https://doi.org/10.1016/j.proci.2020.08.062

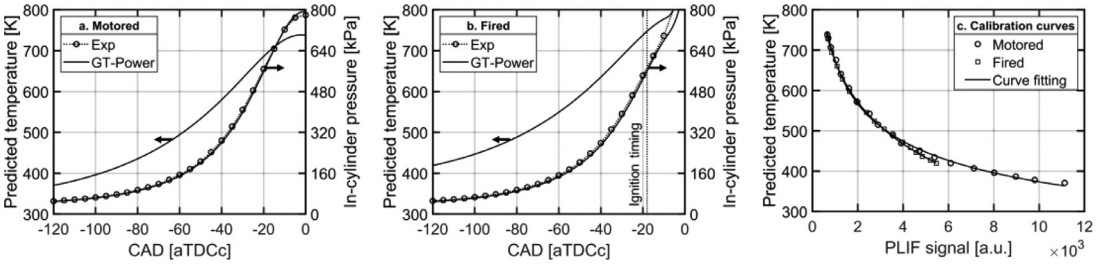

Fig. 2. In-cylinder pressure measurements and predicted temperatures and pressures from GT-Power for (a) motored and (b) fired operation conditions, along with (c) the calibration curves.

multi-cycle mean PLIF image was done to correct for laser attenuation and other non-uniformities. A moving Gaussian filter to a window of 92×92 pixel^2 (1×1 mm^2) was applied lastly to the fluorescence images before temperature calibration for noise reduction, and to match the mesh resolution of the accompanying LES (described in Section 3). Background signal in the very near-wall proximity due to reflections prevented reporting any temperature measurements closer than 0.5 mm from the wall, and no results are presented after ignition timing under fired conditions due to OH* chemiluminescence background signal from the combustion event.

The spatial average PLIF signal was extracted from a 1×1 mm^2 calibration region in the multi-cycle mean images at a distance of 4 mm from the surface. This distance was chosen to avoid the effects of the near-wall flow and represent the bulk gas temperature, as assessed in the accompanying LES work in [27]. PLIF signals at each CAD during the compression stroke were then calibrated to predicted in-cylinder temperatures from a 1-D GT-Power simulation tuned to match the experimental pressures within ±5% error, as shown in Fig. 2.

Temperature sensitivity of toluene PLIF is recognized to be significantly less in the presence of oxygen due to the effects of quenching [28], which is taken into account within the temperature calibration curve. Random errors originating from intensifier shot noise and variations in laser intensity are the primary sources for precision uncertainty of the PLIF thermometry technique [8,10,12–14] The PLIF uncertainty was defined as the ratio of standard deviation to the ensemble-average PLIF signal [14], and the corresponding temperature uncertainty was determined from the spatial deviation of temperature fluctuations. PLIF precision uncertainty was found to be less than ±8% within the calibration region, while the temperature uncertainty was ±1.5 K. Larger precision uncertainty occurred closer to TDC due to relatively lower SNR and lower sensitivities at higher temperatures [10,12–14].

3. Numerical method

A commercial CFD software (CONVERGE v.2.4.18) was used to perform LES under motored conditions. Simulations for fired conditions are underway. Conjugate heat transfer (CHT) was used to obtain the surface temperature at the fluid-solid interface. CHT solves the coupled heat transfer between fluid and solid domains, which removes the uncertainty associated with the solid-fluid interface thermal boundary conditions. More details of the numerical model setup and its validation for the bulk flow can be found in [17], while a brief description of the numerical method is given here.

Turbulence at the subgrid scale was modeled using the dynamic structure model. The momentum and thermal boundary layers were modeled using the Werner and Wengle model [29] and the Han and Reitz model [30], respectively. The wall models were implemented in the first cell at the fluid-solid interface using the models' original constants. The computational domain includes the exhaust and intake plenums, ports, and the cylinder, and solid geometries (cylinder head, cylinder liner, valves and valve seats, full spark plug geometry, and piston) were included. Orthogonal cubic meshes are used during run-time, with a base mesh of 8 mm, with finer grids within the combustion chamber, where the mesh gradually reduced to 1 mm. A 0.5 mm mesh between solid-solid and fluid-solid interfaces was used.

Inlet and outlet boundary conditions were obtained from GT-Power, following [31], with intake temperature controlled at 353 K. The temperature at the cylinder head top and groove, and valve stems was set to 353 K. Convective boundary condition was applied to the exposed sides and bottom of the cylinder head, with heat transfer coefficient $h = 10$ W/m^2-K and ambient temperature of 298 K. The piston skirt, liner bottom, and inner liner surface was set to adiabatic. The piston bottom and liner outer surface are exposed to cooling air jet, and a convective boundary condition is applied with $h = 200$ W/m^2-K and temperature of 298 K.

Please cite this article as: M.K. Alzuabi, A. Wu and V. Sick, Experimental and numerical investigation of temperature fluctuations in the near-wall region of an optical reciprocating engine, Proceedings of the Combustion Institute, https://doi.org/10.1016/j.proci.2020.08.062

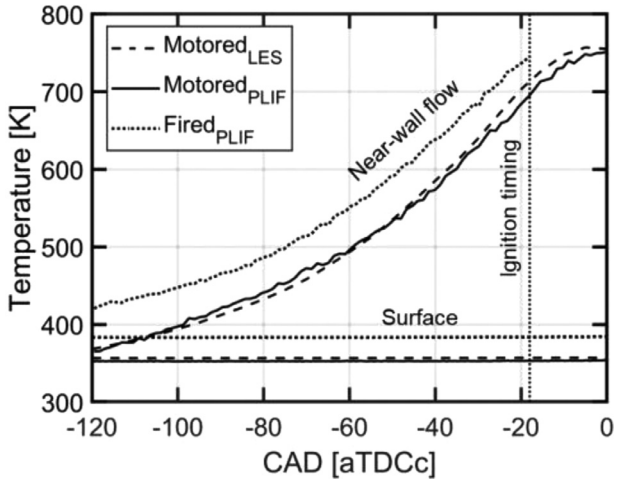

Fig. 3. Temperature rise in the NWR during compression under motored and fired conditions.

A separate liquid coolant simulation was performed for the coolant jacket in the cylinder head using RANS RNG k-ε turbulence model [32] with adaptive mesh refinement, and scalable wall function [33]. A mixture of 50:50 by volume of ethylene glycol and water was fed through the inlet at 3.15×10^{-4} m/s and at 353 K. Initially, the coolant wall temperature was uniformly 353 K. This simulation provides a spatially varying convective boundary condition for the CHT model. The CHT model was then run with the RANS RNG k-ε turbulence model [32] to update the coolant wall temperature. This iteration was done three times for converged convective boundary condition at the coolant wall. The RANS-CHT model provided the initial condition for the first LES cycle. 11 consecutive LES cycles were simulated, with the first cycle was removed to prevent initial condition bias.

4. Results and discussion

In this study, temperature fluctuations are defined about the multi-cycle mean, following common practice in literature. These fluctuations increase during compression as a result of increasing temperature difference between the in-cylinder flow and the cooled walls [34]. Figure 3 shows the rise of the gas temperature in the NWR under motored and fired conditions, alongside the temperature of the in-cylinder head surface at the heat flux probe location. These temperatures are the spatial average value of the multi-cycle mean temperature distributions extracted from the 8×6 mm^2 FoV. Numerical results are in a good agreement with measurements under motored conditions in terms of capturing the temperature rise in the NWR and predicting the surface temperature, mainly due to the inclusion of the CHT model [17].

Figure 4 presents instantaneous images of temperature fluctuations during the compression stroke, and each row represents a temporal sequence of a single-cycle, with the first row showing results from LES, and second and third rows showing PLIF results under motored and fired conditions. Instantaneous temperature fluctuations prior to ignition during the compression stroke are valuable to examine due to their impact on numerous aspects in SI engines including the mixture preparation, auto-ignition, flame propagation, heat losses, and pollution formation [14]. The findings are also relevant to HCCI engines since such fluctuations affect the combustion phasing and maximum peak release rate [9,10]. Increasing thermal stratification towards TDC is evident by the increasing number of fluctuating temperature regions and their temperature difference. Thermal stratification appears to be similar under motored and fired conditions prior to combustion in this engine, which agrees with [9]. Numerical results do not capture any significant stratification in the NWR during early compression, but show higher temperature fluctuations during late compression.

The repeatability of patterns observed in the instantaneous images is assessed by inspecting the multi-cycle standard deviation (not shown) [8]. Multi-cycle standard deviation values increase with compression due to increasing fluctuations, and the regions of the largest cycle-to-cycle temperature fluctuations, as outlined by the dashed lines on Fig. 4, are closer to the in-cylinder head surface where high thermal gradients are expected to occur. The dashed lines represent 65% of the maximum multi-cycle standard deviation value at each CAD. This further confirms the unsteadiness of the thermal boundary layer at the in-cylinder head as observed in [10].

Please cite this article as: M.K. Alzuabi, A. Wu and V. Sick, Experimental and numerical investigation of temperature fluctuations in the near-wall region of an optical reciprocating engine, Proceedings of the Combustion Institute, https://doi.org/10.1016/j.proci.2020.08.062

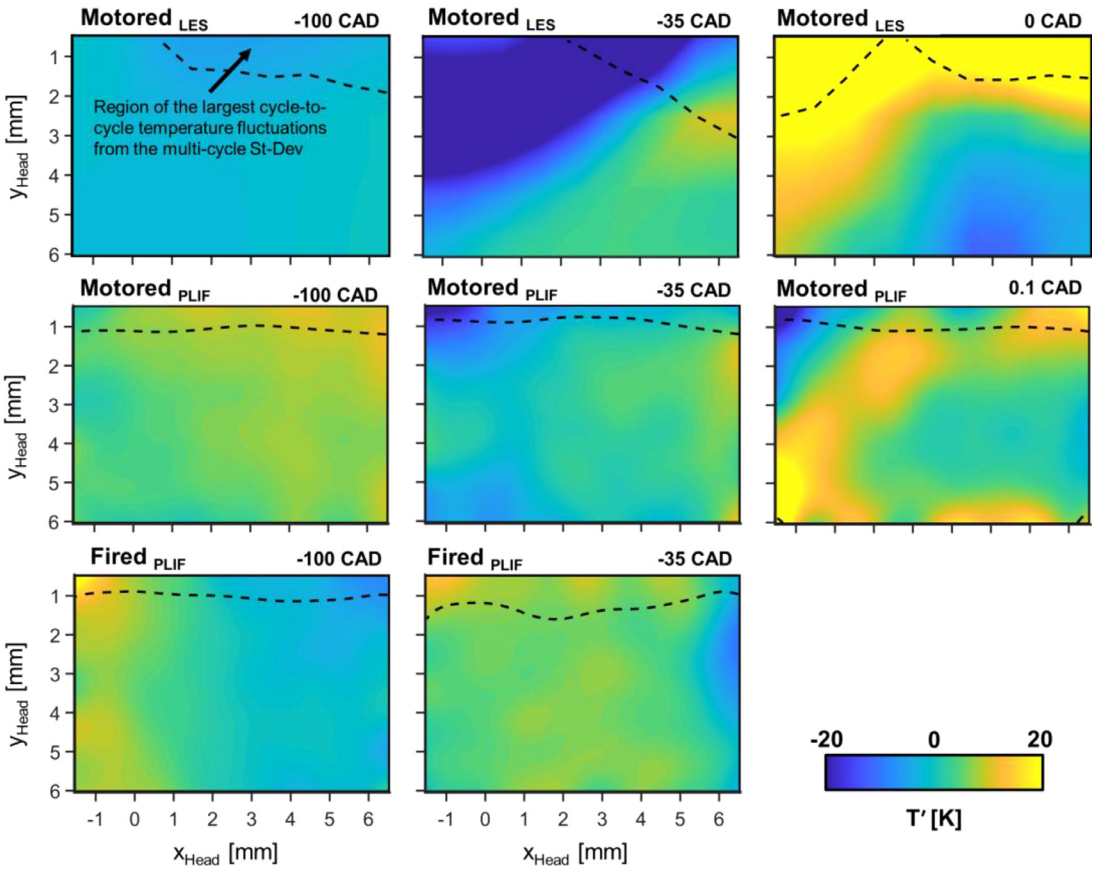

Fig. 4. Temporal evolution of thermal stratification in the NWR during compression under motored and fired conditions. Regions of the largest cycle-to-cycle temperature fluctuations, indicated by the highest multi-cycle St-Dev, are confined in-between the in-cylinder head surface and the dashed lines.

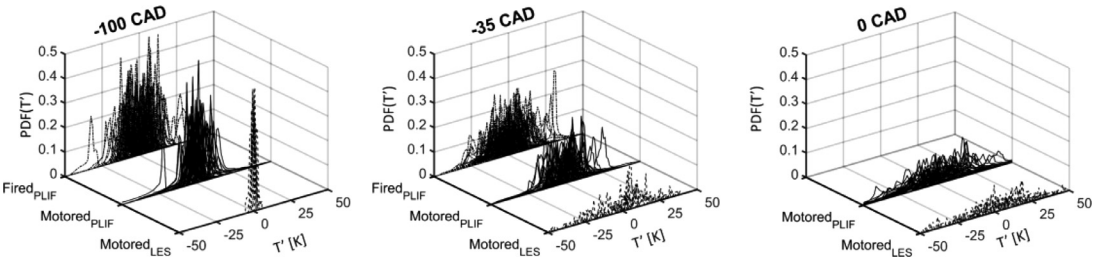

Fig. 5. PDFs of fluctuating temperature in the NWR (each curve represents a single cycle).

Temperature fluctuations about the multi-cycle mean include effects of turbulence and CCV [35]. To further assess their cyclic variability, Fig. 5 presents probability density functions (PDFs) of near-wall temperature fluctuations for multiple consecutive cycles. While these PDFs describe temperature fluctuations in the NWR, they reveal similar effects of compression on in-cylinder temperature as reported in [21]. The PDF (T') transitions from narrow distributions with pronounced peaks during early compression, indicating low temperature fluctuations, to wide and dispersed at the end of compression due to increasing wall heat losses. The curves appear to be skewed and multimodal as a result of interaction with colder near-wall fluid in the NWR [8,21]. The spread of fluctuating temperatures appears to be similar under motored and fired conditions. Numerical results follow the same

Please cite this article as: M.K. Alzuabi, A. Wu and V. Sick, Experimental and numerical investigation of temperature fluctuations in the near-wall region of an optical reciprocating engine, Proceedings of the Combustion Institute, https://doi.org/10.1016/j.proci.2020.08.062

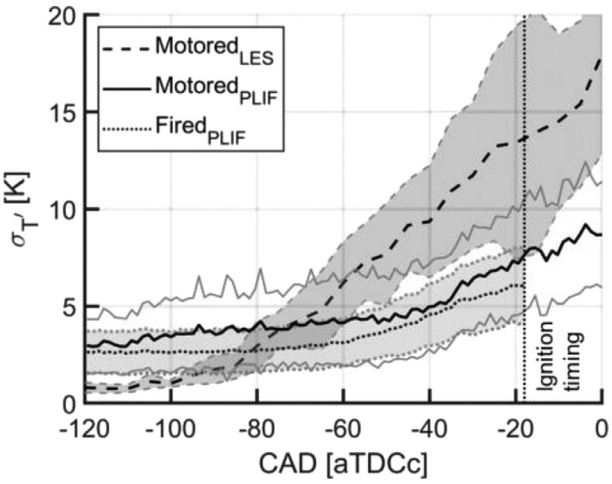

Fig. 6. Evolution of fluctuating thermal stratification in the NWR.

trend but show less fluctuations than measurements during early compression.

Thermal stratification is expected to develop across the in-cylinder core region during late compression, when the bulk-gas temperature has risen well above the wall temperature [8,9]. However, stratification in the NWR is likely to develop earlier during compression because of closer interaction with colder gases. Figure 6 presents the spatial standard deviation of fluctuating temperatures in the NWR. It quantifies the magnitude of the fluctuating thermal stratification ($\sigma_{T'}$) during compression caused by random penetration of turbulent cold structures into the NWR [8]. Lines and shaded areas represent the multi-cycle mean and standard deviation values, respectively. Experimental results exhibit early fluctuations in the compression stroke with a gradual rise towards TDC. Fluctuating stratification is marginally higher under motored conditions than fired, which could be due to differences in turbulent convective transport of colder near-wall gases. Numerical results show minimal fluctuations early in the compression stroke, but a steep rise after -90 CAD leading to higher fluctuations than measurements during late compression.

Spatial correlation analysis of temperature fluctuations in the NWR is valuable for validating wall heat transfer models. It provides insights into the spatial scale of fluctuating temperature structures [8] and describe near-wall thermal gradients [20,21]. Moreover, it could be used to identify the extent of the wall boundary effect [18]. Figure 7 presents single-sided, two-point spatial correlation coefficients of temperature fluctuations in the wall-normal direction for the correlation point $y_{\mathrm{Head}} = 0.5$ mm, following the method described in [18]. Lines and shaded areas represent the average and standard deviation over the wall-parallel direction (x_{Head}). Results show strong correlations in the near-wall proximity where the largest cycle-to-cycle temperature fluctuations are confined, but they experience an initial drop outside of the buffer layer, identified in [19,23]. Correlations under fired conditions are stronger, indicating larger integral length scales and less thermal gradients in the NWR compared to motored conditions. This is commensurate with velocity measurements that show higher fluctuations in the NWR for fired operation [19], which would help to decrease thermal gradients through mixing enhancement. Also, they vary less in the wall-parallel direction, indicated by the shaded areas, in contrast to the motored conditions. Correlations from LES experience a stronger initial drop within the NWR, at the same wall distance, pointing to smaller temperature length scales in the simulations compared to the measurements. In general, these correlations remain statistically dependent within the NWR, which necessitates a larger imaging field to extract meaningful integral length scales for cross-comparison with DNS results reported by Schmitt et al. [20,34]. Their work investigated fluctuations around the spatial mean, and revealed decreasing temperature length scale towards the wall at TDC due to increasing thermal gradients.

Residual gases under fired operation are expected to have minimal impact on the development of thermal stratification during late compression, assuming residual mixing and low residual gas fraction (~10%). The lower magnitudes of thermal stratification under fired operation could be mainly attributed to higher wall temperatures [36].

Sources of discrepancy between the LES and PLIF results under motored conditions in the NWR were assessed in [27], and are attributed to several modeling factors and experimental inaccuracies. The LES results are dependent on the wall models, the subgrid scale model, the numerical

Please cite this article as: M.K. Alzuabi, A. Wu and V. Sick, Experimental and numerical investigation of temperature fluctuations in the near-wall region of an optical reciprocating engine, Proceedings of the Combustion Institute, https://doi.org/10.1016/j.proci.2020.08.062

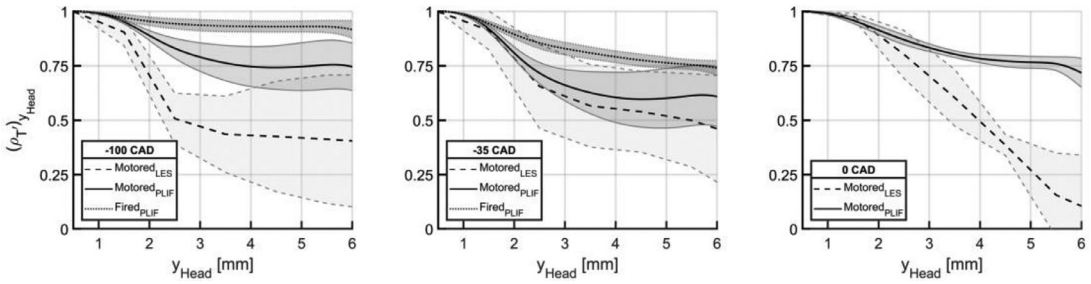

Fig. 7. Two-point spatial correlations of temperature fluctuations in the wall-normal direction. Lines and shaded areas represent the average and spatial standard deviation values in the wall-parallel direction, respectively.

scheme, and the grid resolution, while the PLIF temperature measurements are influenced by the accuracy of the temperature calibration, any local PLIF signal variations caused by inhomogeneous toluene mixture, in addition to any background fluorescence signal due to reflections. However, the overall trend in the spatial correlations of the PLIF temperature fluctuations is captured in the LES.

5. Conclusions

This work investigated near-wall temperature fluctuations in the TCC-III engine using a combined PLIF thermometry and numerical CHT modeling approach. It captured the development of thermal stratification in the NWR during compression under motored and fired conditions. Instantaneous fluctuating temperature fields showed good agreement between numerical and experimental results in terms of increasing thermal stratification towards TDC. Largest cycle-to-cycle temperature fluctuations were identified closer to the in-cylinder head surface indicating the unsteadiness of the thermal boundary layer. PDFs of near-wall temperature fluctuation provided an assessment of the cyclic variability, in addition to capturing the effects of compression on temperature fluctuations. Thermal stratification under motored and fired conditions were similar before ignition timing. Lastly, spatial correlations of temperature fluctuations in the wall-normal direction provided an indication of their spatial scales. It revealed strong correlations in the near-wall proximity that remained statistically dependent in the NWR. Interestingly, these correlations are higher under fired conditions, compared to motored conditions, indicating larger temperature length scales. This is due to higher bulk-gas temperatures and velocity fluctuations as observed in previous near-wall PIV measurements.

Temperature fluctuations about the multi-cycle mean were investigated following common practice in the literature and implementations in models. These describe the cycle-to-cycle thermal gradients, and are important for understanding the effects of the wall boundary layer on the variability of temperature fluctuations. However, it is important to note that spatial temperature gradients drive the heat flux, not the cycle-to-cycle gradients. Thus, it would be valuable to investigate temperature fluctuations about the spatial mean temperature of each individual image, to better characterize engine heat transfer in the NWR.

Declaration of Competing Interest

None.

Acknowledgments

This material is based upon work funded by the Kuwait Foundation for the Advancement of Sciences (KFAS) under project code CB18-65EM-01, the National Science Foundation under the Grant CBET 1402707, "Volumetrically resolved single-shot single-access-point imaging of translucent objects," and the associated INTERN program, as well as the GM-UM Collaborative Research Laboratory, Engine Systems Division. The authors greatly appreciate Convergent Science for their technical support and for providing CONVERGE licenses to the University of Michigan.

References

[1] G. Borman, K. Nishiwaki, *Prog. Energy Combust.* 13 (1987) 1–46.
[2] J.B. Heywood, *Internal Combustion Engine Fundamentals*, McGraw-Hill Book Company, United States, 1988.
[3] J. Chang, O. Güralp, Z. Filipi, D. Assanis, T.-W. Kuo, P. Najt, R. Rask, SAE Technical Paper 2004-01-2996, (2004).
[4] D.L. Reuss, T.W. Kuo, G. Silvas, V. Natarajan, V. Sick, *Int. J. Engine Res.* 9 (2008) 409.
[5] R.P. Lucht, M.A. Maris, SAE Technical Paper 870459, (1987).
[6] R.P. Lucht, D. Dunn-Rankin, T. Walter, T. Dreier, S.C. Bopp, SAE Technical Paper 910722, (1991).

Please cite this article as: M.K. Alzuabi, A. Wu and V. Sick, Experimental and numerical investigation of temperature fluctuations in the near-wall region of an optical reciprocating engine, Proceedings of the Combustion Institute, https://doi.org/10.1016/j.proci.2020.08.062

[7] D. Foster, P.O. Witze, SAE Technical Paper 872105, (1987).
[8] J.E. Dec, W. Hwang, *SAE Int. J. Engines* 2 (2009) 421.
[9] J. Snyder, N. Dronniou, J.E. Dec, R. Hanson, *SAE J. Article 2011-01-1291* 4 (2011) 1669.
[10] N. Dronniou, J. Dec, SAE Technical Papers 2012-01-1111, 5 (2012) 1046.
[11] M.E. Cundy, V. Sick, in: CI/CS Spring Technical Meeting, 2012, pp. Paper # 02-001.
[12] S.A. Kaiser, M. Schild, C. Schulz, *Proc. Combust. Inst.* (2013) 2911–2919.
[13] B. Peterson, E. Baum, B. Böhm, V. Sick, A. Dreizler, *Proc. Combust. Inst.* (2013) 3653–3660.
[14] B. Peterson, E. Baum, B. Bohm, V. Sick, A. Dreizler, *Appl. Phys. B – Lasers O* 117 (2014) 151–175.
[15] A.C. Alkidas, J.P. Myers, *J. Heat Transf.* 104 (1982) 62–67.
[16] A. Misdariis, O. Vermorel, T. Poinsot, *Combust. Flame* 162 (2015) 4304–4312.
[17] A. Wu, S. Keum, V. Sick, *Oil Gas Sci. Technol. – Rev. IFP Energies Nouvelles* 74 (2019).
[18] J.R. Macdonald, C.M. Fajardo, M. Greene, D. Reuss, V. Sick, SAE Technical Paper 2017-01-0613, (2017).
[19] M.L. Greene, PhD thesis, University of Michigan, Ann Arbor, Michigan, USA, 2017.
[20] M. Schmitt, C.E. Frouzakis, Y.M. Wright, A.G. Tomboulides, K. Boulouchos, *Int. J. Engine Res.* 17 (2015) 63–75.
[21] M. Schmitt, C.E. Frouzakis, A.G. Tomboulides, Y.M. Wright, K. Boulouchos, *Proc. Combust. Inst.* (2015) 3069–3077.
[22] P. Schiffmann, S. Gupta, D. Reuss, V. Sick, X. Yang, T.W. Kuo, *Oil Gas Sci. Technol. – Rev. IFP Energies Nouvelles* 71 (2015) 27.
[23] P.C. Ma, M. Greene, V. Sick, M. Ihme, *Int. J. Engine Res.* 18 (2017) 15.
[24] C. Cierpka, S. Scharnowski, C.J. Kähler, *Appl. Opt.* 52 (2013) 2923–2931.
[25] B. Peterson, E. Baum, B. Böhm, V. Sick, A. Dreizler, *Appl. Phys. B* 117 (2014) 151–175.
[26] V. Sick, *Proc. Combust. Inst.* 34 (2013) 3509–3530.
[27] A. Wu, M.K. Alzuabi, V. Sick, SAE Technical Paper 2020-01-1106, (2020).
[28] C. Schulz, V. Sick, *Prog. Energy Combust.* 31 (2005) 75–121.
[29] H. Werner, H. Wengle, Springer Berlin Heidelberg, Berlin, Heidelberg, 1993, pp. 155–168.
[30] Z. Han, R.D. Reitz, *Int. J. Heat Mass Transf.* 40 (1997) 613–625.
[31] T.W. Kuo, X. Yang, V. Gopalakrishnan, Z. Chen, *Oil Gas Sci. Technol.* 69 (2014) 61–81.
[32] V. Yakhot, S.A. Orszag, *J. Sci. Comput.* 1 (1986) 3–51.
[33] K. Richards, P.K. Senecal, E. Pomraning, *CONVERGE v2.4 Manual*, Convergent Science, Inc., Madison, WI, 2018.
[34] M. Schmitt, C.E. Frouzakis, A.G. Tomboulides, Y.M. Wright, K. Boulouchos, *Proc. Combust. Inst.* 35 (2015) 3069–3077.
[35] Funk, V. Sick, D.L. Reuss, W.J.A. Dahm, SAE Technical Paper 2002-01-2841, (2002).
[36] J. Snyder, N. Dronniou, J.E. Dec, R. Hanson, *SAE Int. J. Engines* 4 (2011) 1669.

Please cite this article as: M.K. Alzuabi, A. Wu and V. Sick, Experimental and numerical investigation of temperature fluctuations in the near-wall region of an optical reciprocating engine, Proceedings of the Combustion Institute, https://doi.org/10.1016/j.proci.2020.08.062